Preprint typeset in JHEP style - HYPER VERSION

Soft gluons away from jets: distribution and correlation

Emil Avsar

Institut de Physique Théorique de Saclay, F-91191 Gif-sur-Yvette, France
E-mail: emil.avsar@cea.fr

Yoshitaka Hatta and Toshihiro Matsuo

Graduate School of Pure and Applied Sciences, University of Tsukuba, Tsukuba, Ibaraki 305-8571, Japan
E-mail: hatta@het.ph.tsukuba.ac.jp, tmatsuo@het.ph.tsukuba.ac.jp

Abstract: Recently, an exact conformal mapping between soft gluons emitted from jets at large angle in e^+e^-–annihilation and those in the BFKL evolution of a high energy hadron has been proposed. We elucidate some remarkable aspects of this correspondence and use them to analytically compute the distribution and correlation of gluons in the interjet region. We also establish the timelike counterpart of Mueller's dipole model and discuss the resulting linear and nonlinear evolution equations.

Keywords: QCD, Jets, Hadronic Colliders.

Contents

1. Introduction

Electron–positron (e^+e^-) annihilation into hadrons is one of the most well–studied high energy reactions that offers a broad arena for testing perturbative QCD predictions [1]. A number of fixed–order and resummed calculations with ever increasing precision have been developed for a variety of observables ranging from jet cross sections to event shape variables. The impressive agreement between these predictions and experiment witnessed over the past few decades undoubtedly represents a major success of perturbative QCD.

While a large fraction of the theoretical activity in e^+e^-–annihilation has been centered around jet–related observables, there is a great deal of physics to be explored in regions *between* jets. A primary example is the energy flow E_{out} [2–6], the total amount of energy radiated into a specified angular region away from the hard jets. The underlying partonic process that pertains to interjet observables is the multiple emission of soft gluons at wide angle. In perturbative calculations, large logarithms, called 'non–global logarithms' [7–15], of the type $(\alpha_s \ln Q/\mathcal{M})^n$ appear, where Q is the center–of–mass energy and $\mathcal{M}$ is a second hard scale $Q \gg \mathcal{M} \gg \Lambda_{QCD}$ characterizing the observable of interest. [$\mathcal{M} = E_{out}$ in the case of energy flow.] These logarithms arise due to emissions from secondary gluons and are therefore sensitive to complicated multi–gluon configurations in interjet regions.

Intertwined with the Sudakov logarithms [6] associated with emissions from the primary hard partons, their resummation is a challenging task in perturbation theory (see, however, [11]).

Initially, the resummation of non–global logarithms to all orders was done numerically, in Monte Carlo simulations in the large–N_c limit [7,8,15]. On the other hand, the authors of [9, 16] have succeeded in resumming logarithms in the form of evolution equations. Very interestingly, their results bear a striking resemblance to the BFKL [17, 18] and the BK [19,20] equations which have been hitherto discussed exclusively in the context of high energy (Regge) scattering. Indeed, the equations in [9] and [16] are almost identical in form to the BK and BFKL equations respectively, after merely replacing the kernel of the evolution equations as

$$\frac{d^2\Omega_c}{4\pi}\frac{1-\cos\theta_{ab}}{(1-\cos\theta_{ac})(1-\cos\theta_{cb})} \to \frac{d^2\boldsymbol{x}_c}{2\pi}\frac{\boldsymbol{x}_{ab}^2}{\boldsymbol{x}_{ac}^2\boldsymbol{x}_{cb}^2}\,. \tag{1.1}$$

Here, the left–hand–side is the well–known radiation function of a soft gluon (labeled c) from parent partons a and b (θ_{ab}, etc. are relative angles between momenta.), whereas the right–hand–side is the dipole splitting probability in impact parameter space ($\boldsymbol{x}$'s are two–dimensional vectors and $\boldsymbol{x}_{ab} \equiv \boldsymbol{x}_a - \boldsymbol{x}_b$) which is the fundamental building block of the dipole formulation of the BFKL equation [21].

Such a resemblance naturally prompts one to seek a possible relationship between the two processes (e^+e^- vs. Regge) at a fundamental level. In [22], it was pointed out that the map (1.1) is a conformal transformation, known as the stereographic projection. Moreover, in the strong coupling limit of $\mathcal{N}=4$ supersymmetric Yang–Mills (SYM) theory the *same* transformation exactly relates the final state in e^+e^-–annihilation and the high energy hadronic wavefunction in impact parameter space. The way this latter result was derived (see [22] for the details) emphasizes that in the soft sector the two processes are one and the same phenomenon, the only difference being the choice of the coordinate system in which to express its physics content. In view of this, the correspondence (1.1) at weak coupling is hardly accidental, but must have a deep geometrical origin that goes beyond the perturbative framework.

The purpose of this paper is to establish a detailed dictionary of the transformation rules and explore its physical consequences. The practical advantage in doing so is that on the BFKL side a number of exact analytical results are known with the help of conformal (or rather, the Möbius) symmetry. Making the most of the dictionary, one can obtain analytical insights which incorporate the effects of the resummation into the partonic final state in e^+e^-–annihilation. We start by in the next section reviewing some basic facts about the stereographic projection which realizes the map (1.1). We clarify how the map correctly accounts for the subtle difference in kinematics between the two processes. Then in Section 3, we discuss the single and double gluon angular distributions and related observables in the interjet region. In Section 4, we construct the exact timelike analog of Mueller's dipole model using the generating functional technique. In light of this, the nonlinear evolution equations in the timelike and spacelike contexts can be treated in a unified fashion. Then in Section 5, we study the correlation of dipoles (heavy–quark pairs)

in the interjet region based on the results in [23, 24]. Finally in Section 6, we look into the small–angle (distance) limit of the energy correlation functions in the dipole model and reproduce the OPE result in [25].

2. Stereographic projection

The stereographic projection is a mapping between the unit sphere with coordinates $\Omega = (\theta, \phi)$ and the two–dimensional plane $\boldsymbol{x} = (x^1, x^2)$. It is defined by the relations

$$x^1 = \frac{\sin\theta\cos\phi}{1+\cos\theta}\,, \quad x^2 = \frac{\sin\theta\sin\phi}{1+\cos\theta}\,, \tag{2.1}$$

or equivalently,

$$\cos\theta = \frac{1-\boldsymbol{x}^2}{1+\boldsymbol{x}^2}, \quad \sin\theta = \frac{2|\boldsymbol{x}|}{1+\boldsymbol{x}^2}, \quad \cos\phi = \frac{x^1}{|\boldsymbol{x}|}, \quad \sin\phi = \frac{x^2}{|\boldsymbol{x}|}\,. \tag{2.2}$$

The squared length transforms as

$$(d\boldsymbol{x})^2 = \frac{1}{(1+\cos\theta)^2}(d\theta^2 + \sin^2\theta d\phi^2) \equiv \frac{1}{(1+\cos\theta)^2} d\Omega^2\,, \tag{2.3}$$

and the area element as

$$d^2\Omega = (1+\cos\theta)^2 d^2\boldsymbol{x} = \frac{4}{(1+\boldsymbol{x}^2)^2} d^2\boldsymbol{x}\,. \tag{2.4}$$

If one thinks of the sphere as being embedded in a three dimensional space (y^1, y^2, y^3), the stereographic map can be viewed as a part of the following conformal transformation in four-dimensions [26];

$$x^+ = -\frac{1}{2y^+}, \quad x^- = y^- - \frac{\boldsymbol{y}^2}{2y^+}, \quad \boldsymbol{x} = \frac{\boldsymbol{y}}{\sqrt{2}y^+}\,, \tag{2.5}$$

where $\boldsymbol{y} = (y^1, y^2)$ and $x^\pm = (x^0 \pm x^3)/\sqrt{2}$, $y^\pm = (y^0 \pm y^3)/\sqrt{2}$.

We shall regard $\boldsymbol{x}$ as the transverse plane perpendicular to the direction of a high energy hadron.[1] The operator which measures the energy density at $\boldsymbol{x}$ is given by

$$\mathcal{E}(\boldsymbol{x}) = \frac{1}{\sqrt{2}}\int_{-\infty}^{\infty} dx^- T_{--}(x^+ = 0, x^-, \boldsymbol{x})\,. \tag{2.6}$$

On the other hand, the coordinates $\Omega = (\theta, \phi)$ are identified with the polar coordinates of quarks and gluons in the final state of e^+e^-–annihilation. The total four–momentum as measured in the y–coordinates is related to $\mathcal{E}(\boldsymbol{x})$ via the following rules [25]

$$P^+ = \sqrt{2}\int d^2\boldsymbol{x}\,\mathcal{E}(\boldsymbol{x}), \tag{2.7}$$

$$P^- = \sqrt{2}\int d^2\boldsymbol{x}\,\boldsymbol{x}^2\mathcal{E}(\boldsymbol{x}), \tag{2.8}$$

$$\boldsymbol{P} = 2\int d^2\boldsymbol{x}\,\boldsymbol{x}\mathcal{E}(\boldsymbol{x})\,. \tag{2.9}$$

[1] In the presence of conformal symmetry, it is natural to define $\boldsymbol{x}$ to be a dimensionless variable. When necessary, one can easily restore the length scale in the problem.

In particular the energy is given by

$$E = \int d^2\Omega\, \mathcal{E}(\Omega) = \frac{1}{\sqrt{2}}(P^+ + P^-) = \int d^2\boldsymbol{x}(1+\boldsymbol{x}^2)\, \mathcal{E}(\boldsymbol{x})\,, \tag{2.10}$$

where the operator [2, 3]

$$\mathcal{E}(\Omega) \equiv \lim_{r\to\infty} r^2 \int_0^\infty dy^0\, n_i T^{0i}(y^0, r\vec{n}) = \frac{2}{(1+\cos\theta)^3}\mathcal{E}(\boldsymbol{x})\,, \tag{2.11}$$

with $\vec{n} = (\sin\theta\cos\phi, \sin\theta\sin\phi, \cos\theta)$ and $r = \sqrt{y_1^2 + y_2^2 + y_3^2}$, measures the total energy flowing into the direction Ω. In (2.11), the factor of 2 accounts for the fact that to a high energy hadron with four–momentum $(E, 0, 0, E)$ in the x–coordinates corresponds a virtual static photon with four–momentum $(Q = 2E, 0, 0, 0)$ in the y–coordinates.

In the following we shall be often interested in the energy and momentum of individual gluons rather than the total four–momentum. The transformation rules (2.7)–(2.9) instruct us to make the identifications

$$\boldsymbol{p} \leftrightarrow 2\boldsymbol{x}\, k^0\,, \tag{2.12}$$

$$p^0 \leftrightarrow (1+\boldsymbol{x}^2)k^0\,, \tag{2.13}$$

where we employ the convention that the four–momentum of gluons in the timelike cascades (the y–coordinates) is denoted by p^μ, while that in the spacelike cascades (the x–coordinates) is denoted by k^μ. [In fact, in the present approach the transverse momentum in the spacelike problem $\boldsymbol{k}$ does not appear explicitly, but only implicitly as the inverse of the transverse coordinates, $\boldsymbol{x} \sim \boldsymbol{k}^{-1}$.] Note that equations (2.12) and (2.13) are not independent of each other due to the identity

$$\frac{|\boldsymbol{p}|}{p^0} = \sin\theta = \frac{2|\boldsymbol{x}|}{1+\boldsymbol{x}^2}\,. \tag{2.14}$$

So far, the stereographic projection (2.1) has been introduced merely as a rule to associate particles living in two different coordinate systems. However, it turns out that this correspondence is preserved by the QCD evolution in the soft approximation. As observed in [22], the differential probability of emitting a soft gluon from a dipole (a quark–antiquark pair) with opening angle θ_{ab}

$$\bar{\alpha}_s \frac{d^2\Omega_c}{4\pi} \frac{1-\cos\theta_{ab}}{(1-\cos\theta_{ac})(1-\cos\theta_{cb})} \equiv \bar{\alpha}_s d^2\Omega_c K_{ab}(\Omega_c), \quad \bar{\alpha}_s = \alpha_s N_c/\pi, \tag{2.15}$$

is exactly mapped via the stereographic projection onto the gluon emission probability from a dipole with transverse size $\boldsymbol{x}_{ab} = \boldsymbol{x}_a - \boldsymbol{x}_b$ in the spacelike process,

$$\bar{\alpha}_s \frac{d^2\boldsymbol{x}_c}{2\pi} \frac{\boldsymbol{x}_{ab}^2}{\boldsymbol{x}_{ac}^2 \boldsymbol{x}_{cb}^2} \equiv \bar{\alpha}_s d^2\boldsymbol{x}_c\, K_{ab}(\boldsymbol{x}_c)\,. \tag{2.16}$$

[Thus we use the same notation K in both cases but from the argument of K it should always be obvious whether we mean (2.15) or (2.16).] This implies that, at least to leading

logarithmic accuracy (and in fact in the large–N_c approximation), the high energy (small Bjorken–x) QCD evolution in the transverse plane is equivalent to the small Feynman–x structure of the interjet parton shower in e^+e^- annihilation. In order to genuinely establish this statement and also to discuss its limitations we must, however, take a closer look into the details of kinematics. Indeed, there is a subtle but conceptually important difference between the two processes which needs to be addressed: When describing parton cascades in e^+e^- annihilation, it is common to use the variable $|\boldsymbol{p}|$ as the evolution parameter: One usually starts with a large value of $|\boldsymbol{p}|$ set by the splitting of the photon into the quark–antiquark pair, and evolves the cascade towards smaller values of $\boldsymbol{p}$ with strong ordering in their magnitude $|\boldsymbol{p}|$. It is then natural to use $Y_t \equiv \ln(E/|\boldsymbol{p}|)$ as the evolution "time". In contrast, in the spacelike parton cascade of a high energy hadron the transverse momentum is more or less constant while one has strong ordering in energy, which in turn implies strong ordering in angle. One can then use either k^0 or the emission angle θ as the evolution parameter with the evolution time $Y_s = \ln(E/k^0)$ or $Y_s = \ln\theta$, and to leading order the two choices should be equivalent. This difference in kinematics is an unavoidable feature of the multiple soft gluon emission in each case [16], and might be regarded as an obstacle against any attempt to find an exact mapping between the two processes. Remarkably, however, the stereographic projection automatically converts the nature of the evolution parameter into the desired form. Indeed, using (2.12) we have

$$Y_t = \ln\frac{E}{|\boldsymbol{p}|} \leftrightarrow \ln\frac{E}{2|\boldsymbol{x}|k^0}\,. \tag{2.17}$$

Due to our identification of $\boldsymbol{x}$ as the inverse transverse momentum $\boldsymbol{k}^{-1}$, the product $|\boldsymbol{x}|k^0 \sim k^0/|\boldsymbol{k}| = 1/\theta$ is indeed a measure of the emission angle, and thus we are lead to the identification $Y_t \leftrightarrow Y_s$. This assures that, to leading logarithmic accuracy, the correspondence works perfectly including the details of kinematics, and the whole machinery developed for the dipole formulation of the BFKL evolution can be used to analyze interjet observables in e^+e^- annihilation, or *vice versa*.

Let us conclude this section with a few additional remarks:

It seems that the correspondence crucially relies on conformal symmetry, and as such, it may not hold, or at least needs to be modified, in the next–to–leading logarithmic (NLL) approximation in QCD where the running coupling effect breaks conformal symmetry. Indeed, as already pointed out in [16] the argument of the running coupling should be $|\boldsymbol{p}|$ and $|\boldsymbol{k}|$ in the two cases, respectively. This does not agree with the rule (2.12) derived from a consideration of conformal symmetry alone. On the other hand, in $\mathcal{N} = 4$ SYM theory which is conformal, there is a good possibility that the correspondence holds to all orders in the soft approximation, as indicated by the fact that it holds exactly in the strong coupling limit [22]. The recent NLL result reported in [27] is very encouraging from this point of view. In Appendix A we transcribe their result to obtain the timelike NLL dipole kernel.

It is worth mentioning that the collinear singularity $|\boldsymbol{p}| \sim \theta \to 0$ in the timelike emission kernel (2.15) maps onto the ultraviolet singularity $|\boldsymbol{x}| \sim 1/|\boldsymbol{k}| \to 0$ of the spacelike emission kernel (2.16). Conversely, the ultraviolet region $|\boldsymbol{p}| \to \infty$ maps onto the collinear region

$|\boldsymbol{k}| \to 0$. Also note that in the timelike case this collinear singularity is responsible for generating angular–ordered gluons surrounding the primary quark and antiquark which eventually materialize into observed jets of hadrons with the multiplicity given by the standard double–logarithmic formula [28]. These collinear gluons are also mapped onto the transverse plane of a high energy hadron via the stereographic projection, although in this latter case they are irrelevant fluctuations which are basically invisible in the scattering process. In Appendix B, as another interesting aspect of this correspondence, we describe the interplay between the boost in the y^μ–frame and the scale transformation (dilatation) in the x^μ–frame originally noted in [25].

3. Interjet gluon distribution

3.1 Single gluon distribution

As a concrete example of the above mapping, let us compute the distribution of a single gluon emitted from a color dipole (a $q\bar{q}$ pair). We begin with the $\boldsymbol{x}$–space and denote by $\boldsymbol{x}_{a(b)}$ the coordinates of the quark (antiquark). The single gluon distribution is

$$\frac{d^2N}{d^2\boldsymbol{x}} = \bar{\alpha}_s K_{ab}(\boldsymbol{x}) \int \frac{dk^0}{k^0} = \bar{\alpha}_s K_{ab}(\boldsymbol{x}) \int_0^{\ln(E/\Lambda)} dY_s \,, \tag{3.1}$$

where $Y_s = \ln \frac{E}{2|\boldsymbol{x}|k^0}$ and Λ is a cutoff.[2] Applying the stereographic projection, we obtain

$$\begin{aligned} \frac{d^2N}{d^2\Omega} &= \frac{1}{(1+\cos\theta)^2} \frac{d^2N}{d^2\boldsymbol{x}} = \bar{\alpha}_s K_{ab}(\Omega) \int_0^{\ln(E/\Lambda)} dY_t \\ &= \frac{\bar{\alpha}_s}{4\pi} \frac{1}{\sin^2\theta} \int_{\Lambda^2}^{E^2} \frac{d\boldsymbol{p}^2}{\boldsymbol{p}^2} \,, \end{aligned} \tag{3.2}$$

where in the last equality we consider the back–to–back jets configuration $\theta_a = 0$, $\theta_b = \pi$, which corresponds to the choice $\boldsymbol{x}_a = 0$, $\boldsymbol{x}_b = \infty$, see figure 1. Note that we have made the substitution $Y_s \to Y_t = \ln(E/|\boldsymbol{p}|)$ following (2.17).

The energy distribution can be similarly computed. In the spacelike case we have

$$\mathcal{E}(\boldsymbol{x}) = \bar{\alpha}_s K_{ab}(\boldsymbol{x}) \int_0^{\ln(E/\Lambda)} k^0 \, dY_s = \bar{\alpha}_s K_{ab}(\boldsymbol{x}) \int_0^{\ln(E/\Lambda)} \frac{Ee^{-Y_s}}{2|\boldsymbol{x}|} \, dY_s \,. \tag{3.3}$$

Using (2.11), we find, for the back–to–back jets,

$$\begin{aligned} \mathcal{E}(\Omega) &= \frac{2}{(1+\cos\theta)^3} \mathcal{E}(\boldsymbol{x}) \\ &= \frac{2}{(1+\cos\theta)^3} \frac{\bar{\alpha}_s}{2\pi} \frac{(1+\cos\theta)^2}{\sin^2\theta} \int \frac{Ee^{-Y_t}}{2\sin\theta/(1+\cos\theta)} dY_t \\ &= \frac{\bar{\alpha}_s}{4\pi} \frac{1}{\sin^3\theta} \int d\boldsymbol{p}^2 \frac{|\boldsymbol{p}|}{\boldsymbol{p}^2} \,, \end{aligned} \tag{3.4}$$

in agreement with [5]. We note, incidentally, that in the $\boldsymbol{x}$ space the energy distribution far away from the parent dipole falls as $\sim 1/|\boldsymbol{x}|^5$ as can be seen in (3.3).

[2] The limits on the Y_s integral would imply $1 > \theta > \Lambda/E$ in terms of the emission angle $\theta \approx |\boldsymbol{k}|/k^0 \sim \Lambda/|\boldsymbol{x}|k^0$.

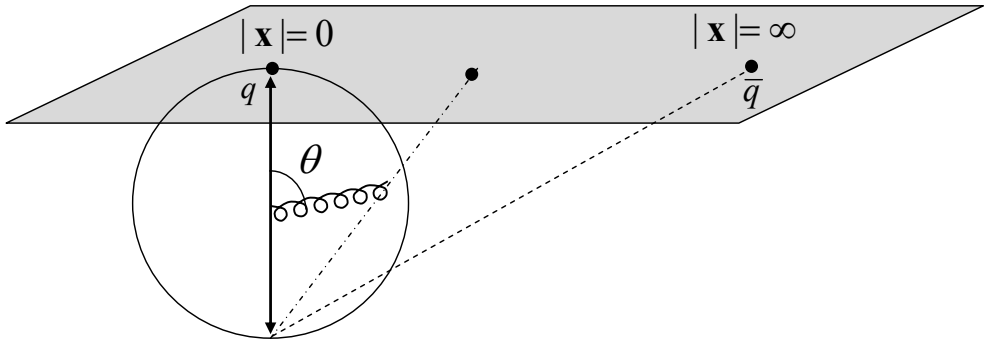

Figure 1: *Stereographic map between the unit sphere and the transverse plane.*

3.2 Resummation to all orders

The results (3.1) and (3.2) can be viewed as the leading order term in the expansion in powers of $\bar{\alpha}_s Y$.[3] If $\bar{\alpha}_s Y$ becomes of order unity, one has to resum all the higher order terms $(\bar{\alpha}_s Y)^n$ consistently. In the spacelike case, this can be done in Mueller's dipole model [21, 29]. In this approach the average total number of dipoles $(\boldsymbol{x}_1, \boldsymbol{x}_2)$ within a rapidity interval Y contained in the parent dipole $(\boldsymbol{x}_a, \boldsymbol{x}_b)$ is given by[4]

$$n_Y(\boldsymbol{x}_{ab}, \boldsymbol{x}_{12}) = \frac{16}{2\pi(\boldsymbol{x}_{12}^2)^2} \sum_n \int_{-\infty}^{\infty} \frac{d\nu}{(2\pi)^3} \left(\nu^2 + \frac{n^2}{4}\right) e^{\bar{\alpha}_s \chi(n,\nu) Y} \times \int d^2\boldsymbol{x}_c E^{1-h,1-\bar{h}}(\boldsymbol{x}_{1c}, \boldsymbol{x}_{2c}) E^{h,\bar{h}}(\boldsymbol{x}_{ac}, \boldsymbol{x}_{bc}) \,, \tag{3.5}$$

where $\chi(n,\nu)$ is the usual BFKL eigenvalue, and $E^{h,\bar{h}}$ is the eigenfunction of the SL(2,$\mathbb{C}$) Casimir operator (see, e.g., [30]) with $h = \frac{1-n}{2} + i\nu$, $\bar{h} = \frac{1+n}{2} + i\nu$.

Formally, the total number of dipoles (equal to the total number of gluons plus one) is given by the integration

$$N_Y = \int d^2\boldsymbol{x}_1 d^2\boldsymbol{x}_2 \, n_Y(\boldsymbol{x}_{ab}, \boldsymbol{x}_{12}) \,. \tag{3.6}$$

As we shall soon see, the integral is actually divergent. Ignoring this fact for the moment, let us analyze its structure from the viewpoint of conformal symmetry. The $d^2\boldsymbol{x}_c$ integration in (3.5) gives a function (see below) only of the anharmonic ratio

$$\rho = \frac{z_{ab} z_{12}}{z_{a1} z_{b2}} = \frac{\left(\tan\frac{\theta_a}{2} e^{i\phi_a} - \tan\frac{\theta_b}{2} e^{i\phi_b}\right)\left(\tan\frac{\theta_1}{2} e^{i\phi_1} - \tan\frac{\theta_2}{2} e^{i\phi_2}\right)}{\left(\tan\frac{\theta_a}{2} e^{i\phi_a} - \tan\frac{\theta_1}{2} e^{i\phi_1}\right)\left(\tan\frac{\theta_b}{2} e^{i\phi_b} - \tan\frac{\theta_2}{2} e^{i\phi_2}\right)} \,, \tag{3.7}$$

[3] In the following we do not distinguish Y_t from Y_s.

[4] Our normalization of n_Y differs from the usual one in the literature by a factor of $1/(2\pi\boldsymbol{x}_{12}^2)$. Note also that despite our somewhat sloppy notation, n_Y in fact depends separately on $\boldsymbol{x}_a$, $\boldsymbol{x}_b$, $\boldsymbol{x}_1$ and $\boldsymbol{x}_2$. The same remark applies to the other distributions to be defined later.

and its complex conjugate. [We have here introduced the complex coordinates $z_a = x_a^1 + ix_a^2$, etc.] The square of this ratio is

$$|\rho|^2 = \frac{\boldsymbol{x}_{ab}^2 \boldsymbol{x}_{12}^2}{\boldsymbol{x}_{a1}^2 \boldsymbol{x}_{b2}^2} = \frac{(1-\cos\theta_{ab})(1-\cos\theta_{12})}{(1-\cos\theta_{a1})(1-\cos\theta_{b2})}\,. \tag{3.8}$$

Moreover, the integration measure

$$\frac{d^2\boldsymbol{x}_1 d^2\boldsymbol{x}_2}{(\boldsymbol{x}_{12}^2)^2} = \frac{d^2\Omega_1 d^2\Omega_2}{4(1-\cos\theta_{12})^2}\,, \tag{3.9}$$

is conformally invariant so that N_Y can be expressed in a manifestly conformally invariant way. Keeping only the $n = 0$ term which is dominant at high energy, we get

$$\begin{aligned} N_Y &= \int d^2\boldsymbol{x}_1 d^2\boldsymbol{x}_2\, n_Y(\boldsymbol{x}_{ab}, \boldsymbol{x}_{12}) = \int \frac{d^2\boldsymbol{x}_1 d^2\boldsymbol{x}_2}{(\boldsymbol{x}_{12}^2)^2} f(\rho,\bar\rho)\,, \\ &\equiv \int d^2\Omega_1 d^2\Omega_2\, n_Y(\Omega_{ab}, \Omega_{12}) = \frac{1}{4}\int \frac{d^2\Omega_1 d^2\Omega_2}{(1-\cos\theta_{12})^2} f(\rho,\bar\rho)\,, \end{aligned} \tag{3.10}$$

where [30, 31]

$$\begin{aligned} f(\rho,\bar\rho) = \int_{-\infty}^{\infty} d\nu\, e^{\bar\alpha_s \chi(\gamma) Y} \Big(& b_\nu |\rho|^{2-2\gamma}\, {}_2F_1(1-\gamma, 1-\gamma, 2-2\gamma; \rho)\, {}_2F_1(1-\gamma, 1-\gamma, 2-2\gamma, \bar\rho) \\ & + b_\nu^* |\rho|^{2\gamma}\, {}_2F_1(\gamma,\gamma,2\gamma;\rho)\, {}_2F_1(\gamma,\gamma,2\gamma;\bar\rho)\Big)\,, \end{aligned} \tag{3.11}$$

with $\gamma \equiv \frac{1}{2} + i\nu = h$, and

$$b_\nu \equiv \frac{\nu 2^{4i\nu}}{2i\pi^3} \frac{\Gamma(\frac{1}{2} - i\nu)\Gamma(1+i\nu)}{\Gamma(\frac{1}{2}+i\nu)\Gamma(1-i\nu)}\,. \tag{3.12}$$

In the second line of (3.10) we are naturally led to define the timelike analog of the single dipole distribution $n_Y(\Omega_{ab}, \Omega_{12})$, that is, the total number of dipoles with opening angle Ω_{12} contained in the parent dipole Ω_{ab} within a rapidity interval Y. A related distribution (integrated over $(\Omega_1 + \Omega_2)/2$) was previously introduced in [16] in the context of the heavy quark pair production in e^+e^-–annihilation. We shall discuss more about this in the next section.

The generalization of the angular distribution (3.2) would be

$$\frac{d^2 N_Y}{d^2\Omega_1} = \frac{(1+\boldsymbol{x}_1^2)^2}{4}\frac{d^2 N_Y}{d^2\boldsymbol{x}_1} = \frac{(1+\boldsymbol{x}_1^2)^2}{4}\, 2\int d^2\boldsymbol{x}_2\, n_Y(\boldsymbol{x}_{ab}, \boldsymbol{x}_{12})\,. \tag{3.13}$$

If we were to assume the $d^2\boldsymbol{x}_2$ (or $d^2\Omega_2$) integral to be convergent, then from dimensional analysis the result would be proportional to

$$\int d^2\boldsymbol{x}_2\, n_Y(\boldsymbol{x}_{ab}, \boldsymbol{x}_{12}) \propto \frac{1}{\boldsymbol{x}_1^2}\,, \tag{3.14}$$

in the limits $\boldsymbol{x}_a \to 0$, $\boldsymbol{x}_b \to \infty$, and therefore,

$$\frac{d^2 N_Y}{d^2\Omega_1} \propto \frac{(1+\boldsymbol{x}_1^2)^2}{4\boldsymbol{x}_1^2} = \frac{1}{\sin^2\theta_1}\,. \tag{3.15}$$

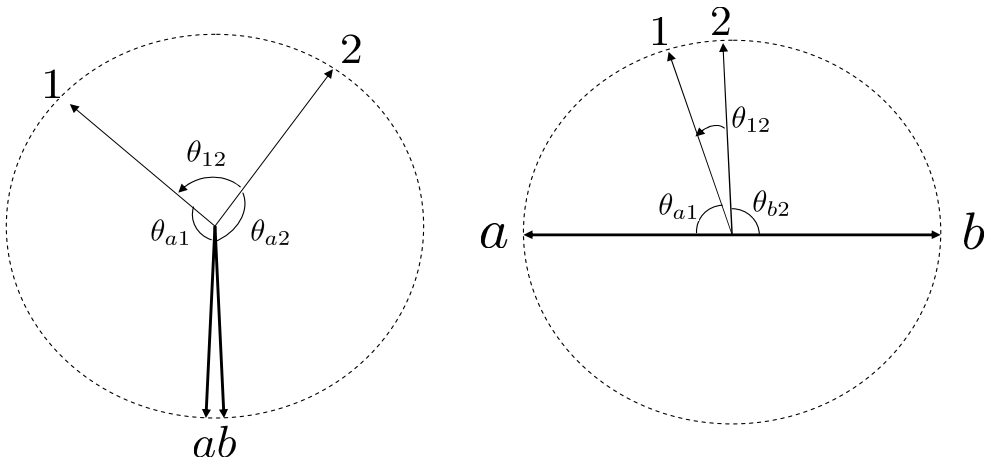

Figure 2: *The angular correlation of gluons in a highly boosted frame of the $q\bar{q}$ pair (left) and in the center–of–mass frame (right).*

This has the same angular dependence $1/\sin^2\theta$ as in the lowest order result (3.2), and in fact it is the unique possibility consistent with boost invariance [5]. However, as already mentioned the integral is divergent due to the singularity at $\boldsymbol{x}_2 = \boldsymbol{x}_1$ (or $\Omega_2 = \Omega_1$). Indeed, when $|\boldsymbol{x}_{12}| \sim \theta_{12}$ is very small, $|\rho|$ is much smaller than unity. We may then approximate as ${}_2F_1(...;\rho) \approx 1$ and find

$$\frac{d^2N_Y}{d^2\Omega_1} \sim \int \frac{d\gamma}{i} \int d^2\Omega_2 \frac{e^{\bar{\alpha}_s\chi(\gamma)Y}}{(1-\cos\theta_{12})^{1+\gamma}}\,. \tag{3.16}$$

For small values of θ_{12}, the anomalous dimension γ at the saddle point is between 0 and $\frac{1}{2}$, hence the singularity is not integrable. It would be interesting to see whether this problem is cured in a more refined treatment including higher order corrections (in particular, the energy conservation) to the BFKL approximation.

On the other hand, the doubly–differential gluon distribution is finite and can be identified with the dipole density itself.[5] When $|\rho| \ll 1$, a simple analytical estimate is possible. This encompasses two physical situations (see fig. 2) which are mathematically equivalent: (i) Radiation from a highly boosted $q\bar{q}$ pair. In this case $\theta_{ab} \ll 1$ and

$$|\rho|^2 \approx \frac{\theta_{ab}^2(1-\cos\theta_{12})}{2(1-\cos\theta_{a1})(1-\cos\theta_{a2})} \ll 1\,. \tag{3.17}$$

Evaluating the γ integral in the saddle point approximation, we find

$$\frac{d^4N_Y}{d^2\Omega_1 d^2\Omega_2} \sim \frac{\theta_{ab}^{2-2\gamma_s}\, e^{\bar{\alpha}_s\chi(\gamma_s)Y}}{(1-\cos\theta_{12})^{1+\gamma_s}(1-\cos\theta_{a1})^{1-\gamma_s}(1-\cos\theta_{a2})^{1-\gamma_s}}\,, \tag{3.18}$$

[5]Some care must be taken in this identification since the two gluons are not selected randomly but are constrained such that they are neighboring in the color space. Though we presume that such a concern is immaterial in the large N_c limit at the level of the two–gluon distribution, the following results may admit somewhat different interpretations such as the measure of color flow at large angle. [Note that even the softest gluons carry color.]

where the saddle point $0 < \gamma_s < \frac{1}{2}$ is determined by the equation

$$\chi'(\gamma_s) = -\frac{1}{\bar{\alpha}_s Y} \ln \frac{1}{|\rho|^2} \,. \tag{3.19}$$

As an example of the value of γ_s, we note that $\gamma_s = 0.47$ for $|\rho|^2 = 0.1$ and $\bar{\alpha}_s Y = 2$. As $|\rho|^2$ decreases further the saddle point moves slowly towards lower values.

(ii) The back–to-back jets case with $\theta_{12} \ll 1$. Setting $\theta_a = 0$, $\theta_b = \pi$ and therefore,

$$|\rho| \approx \frac{\theta_{12}}{\sin\theta_1} \ll 1 \,, \tag{3.20}$$

we obtain

$$\frac{d^4 N_Y}{d^2\Omega_1 d^2\Omega_2} \sim \frac{e^{\bar{\alpha}_s \chi(\gamma_s) Y}}{\theta_{12}^{2+2\gamma_s} (\sin\theta_1)^{2-2\gamma_s}} \,, \tag{3.21}$$

where the saddle point is again given by (3.19).

When θ_{12} becomes large, $|\rho|$ reaches values of order unity. In this regime the hypergeometric function ${}_2F_1(...;\rho)$ has to be fully retained. As an example, let us consider the azimuthal correlation of two gluons around the jet axis by taking $\Omega_a = (0,0)$, $\Omega_b = (\pi, 0)$, $\Omega_1 = (\frac{\pi}{2}, 0)$ and $\Omega_2 = (\frac{\pi}{2}, \phi)$. Equation (3.7) becomes

$$\rho = 1 - e^{i\phi} \,, \qquad |\rho|^2 = 2(1 - \cos\phi) \,. \tag{3.22}$$

This leads to

$$\frac{d^4 N_Y}{d^2\Omega_1 d^2\Omega_2} = 4 \int_{-\infty}^{\infty} d\nu \frac{b_\nu e^{\bar{\alpha}_s \chi(\gamma) Y}}{|\rho|^{2+2\gamma}} \, {}_2F_1(1-\gamma, 1-\gamma, 2-2\gamma; \rho) \, {}_2F_1(1-\gamma, 1-\gamma, 2-2\gamma, \bar{\rho}) \,. \tag{3.23}$$

We have numerically integrated the right–hand–side of (3.23). The result is shown in fig. 3 as a function of ϕ for two different values of $\bar{\alpha}_s Y$. We see that the strong correlation in the collinear direction $\theta_{12} = \phi \ll 1$ as described by (3.21) decreases towards the backward direction and eventually reaches a minimum at $\phi = \pi$.

Another interesting physical quantity is the (pseudo–)rapidity correlator of gluons in the interjet region. The rapidity here is defined as

$$\eta = \ln \cot \frac{\theta}{2} \,, \tag{3.24}$$

in terms of which the anharmonic ratio reads

$$\rho = 1 - \cot\frac{\theta_1}{2} \tan\frac{\theta_2}{2} e^{i(\phi_2 - \phi_1)} = 1 - e^{\eta} e^{i\phi} \,. \tag{3.25}$$

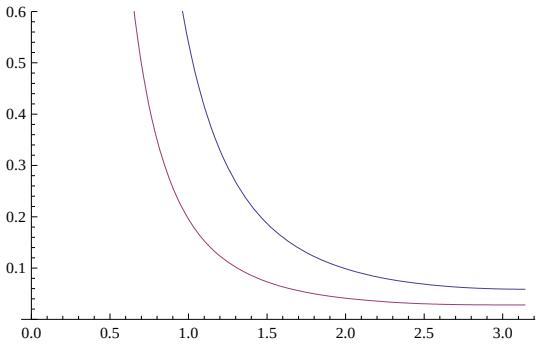

Figure 3: *The azimuthal correlation of two gluons around the jet axis for $\bar{\alpha}_s Y = 2$ (upper curve) and $\bar{\alpha}_s Y = 1.5$ (lower curve). The horizontal axis is $\phi = \theta_{12}$.*

The appearance of the relative rapidity $\eta = \eta_1 - \eta_2$ is a consequence of boost invariance [5]. Integrating (3.23) over the azimuthal angle, we get[6]

$$\frac{d^4 N_Y}{d\cos\theta_1 d\cos\theta_2} = 8\pi \int_0^{2\pi} d\phi \int_{-\infty}^{\infty} d\nu \frac{b_\nu e^{\bar{\alpha}_s \chi(\gamma) Y}}{|\rho|^{2+2\gamma}} \times {}_2F_1(1-\gamma, 1-\gamma, 2-2\gamma; \rho)\, {}_2F_1(1-\gamma, 1-\gamma, 2-2\gamma, \bar{\rho})\,. \quad (3.27)$$

The large η behavior of the above integral can be estimated as follows. We use the identity

$${}_2F_1(\alpha, \alpha, 2\alpha, \rho) = \frac{2^{2\alpha}}{\sqrt{\pi}\Gamma(\alpha)} \Gamma(\alpha + 1/2)(-\rho)^{-\alpha} Q^0_{\alpha-1}(1 - 2/\rho), \quad \rho \notin (0,1), \quad (3.28)$$

where Q^μ_ν is the Legendre function of the second kind. Since $|\rho| \approx e^\eta \gg 1$, we can neglect the ρ dependence of the Legendre function. [Strictly speaking this function goes to an infinite constant in the $\rho \to \infty$ limit.] Using $\alpha = 1 - \gamma$ in our case, we get

$$\frac{d^4 N_Y}{d\cos\theta_1 d\cos\theta_2} \sim \int d\gamma \frac{1}{|\rho|^{2+2\gamma}} \frac{1}{|\rho|^{2-2\gamma}} I(\gamma, Y) = \frac{1}{|\rho|^4} \times I(Y)\,, \quad (3.29)$$

where $I(Y)$ is the value of the η–independent integral. We thus see that at large η the correlator decays as $e^{-4\eta}$. Fig. 4 is the result of a numerical integration of (3.27) as a function of η. The correlator indeed shows an exponential decay $e^{-c\eta}$ with $c \approx 4$ already when $\eta \gtrsim 1$, more or less independently of the value of $\bar{\alpha}_s Y$. In comparison, we note that the energy correlation function in the lowest order (two–gluon) approximation exhibits a similar exponential decay with $c = 3$ [5].

[6] It is physically obvious that the correlator should be invariant under the sign flip $\eta \to -\eta$, thus it is a function only of $|\eta|$, or rather, $e^\eta + e^{-\eta} = 2\cosh\eta$. In (3.27), this can be seen by using an identity of the hypergeometric function

$${}_2F_1(\alpha, \beta, \gamma, z) = (1-z)^{-\alpha}\, {}_2F_1\left(\alpha, \gamma - \beta, \gamma, \frac{z}{z-1}\right), \quad (3.26)$$

or more easily by choosing $\Omega_a = (\pi, 0)$, $\Omega_b = (0, 0)$.

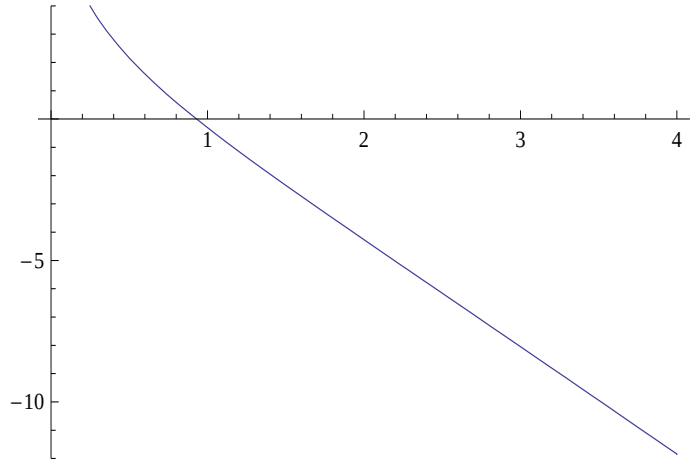

Figure 4: *Logarithm of the right–hand–side of (3.27) for $\bar{\alpha}_s Y = 2$ as a function of η.*

4. Equivalence of the dipole formulations

The single dipole distribution $n_Y(\Omega_{ab}, \Omega_{12})$ defined and studied in the previous section is the exact timelike counterpart of the spacelike distribution $n_Y(\boldsymbol{x}_{ab}, \boldsymbol{x}_{12})$. In this section we show that this correspondence can be generalized to the complete equivalence of the dipole formulation of the timelike and spacelike cascades. The generating functional in Mueller's dipole model is given by

$$Z_{ab}[u, Y] = \sum_{n=1}^{\infty} \int \left(\prod_{i=1}^{n-1} d^2\boldsymbol{x}_i \right) P_n(\boldsymbol{x}_1, \cdots \boldsymbol{x}_{n-1}; Y) u_1 u_2 \cdots u_n \,, \tag{4.1}$$

where $u_i = u(\boldsymbol{x}_{i-1}, \boldsymbol{x}_i)$ is an arbitrary 'weight' function for the i–th dipole and $(\boldsymbol{x}_0, \boldsymbol{x}_n) \equiv (\boldsymbol{x}_a, \boldsymbol{x}_b)$ is the parent dipole. The function P_n is the probability distribution to have n dipoles in a cascade evolved up to rapidity Y. From probability conservation, $Z[u = 1] = 1$. The equation satisfied by P_n is

$$\begin{aligned} \partial_Y P_n(\boldsymbol{x}_1, \cdots \boldsymbol{x}_{n-1}; Y) = &-\bar{\alpha}_s \sum_{i=1}^{n} \int d^2\boldsymbol{z}\, K_{i-1,i}(\boldsymbol{z}) P_n(\boldsymbol{x}_1, \cdots, \boldsymbol{x}_{n-1}; Y) \\ &+\bar{\alpha}_s \sum_{i=1}^{n-1} K_{i-1,i+1}(\boldsymbol{x}_i) P_{n-1}(\boldsymbol{x}_1, \cdots \boldsymbol{x}_{i-1}, \boldsymbol{x}_{i+1}, \cdots \boldsymbol{x}_{n-1}; Y) \,. \end{aligned} \tag{4.2}$$

This has a simple physical interpretation as a gain–loss type of equation. The first term on the right hand side is the "loss" term and describes the total probability for the dipole configuration to disappear via all available decay channels. The second term is the "gain" term which is the probability to obtain the given n-dipole configuration from all possible $n-1$ dipole configurations. The single dipole density is calculated from Z_{ab} via

$$n_Y(\boldsymbol{x}_{ab}, \boldsymbol{x}_{12}) = \left. \frac{\delta Z_{ab}[u, Y]}{\delta u(\boldsymbol{x}_1, \boldsymbol{x}_2)} \right|_{u=1} \,, \tag{4.3}$$

and it obeys the BFKL equation

$$\partial_Y n_Y(\boldsymbol{x}_{ab},\boldsymbol{x}_{12}) = \bar{\alpha}_s \int d^2\boldsymbol{x}_c\, K_{ab}(\boldsymbol{x}_c)\big[n_Y(\boldsymbol{x}_{ac},\boldsymbol{x}_{12}) + n_Y(\boldsymbol{x}_{cb},\boldsymbol{x}_{12}) - n_Y(\boldsymbol{x}_{ab},\boldsymbol{x}_{12})\big]$$
$$\equiv \bar{\alpha}_s \int d^2\boldsymbol{x}_c\, K_{ab}(\boldsymbol{x}_c) \otimes n_Y(\boldsymbol{x}_{ab},\boldsymbol{x}_{12})\,. \tag{4.4}$$

On the other hand, the evolution equation for the generating functional is[7]

$$\partial_Y Z_{ab} = \bar{\alpha}_s \int d^2\boldsymbol{x}_c\, K_{ab}(\boldsymbol{x}_c)(-Z_{ab} + Z_{ac}\, Z_{cb})\,. \tag{4.5}$$

In particular, if one chooses $u(\boldsymbol{x}_{i-1},\boldsymbol{x}_i) = s(\boldsymbol{x}_{i-1},\boldsymbol{x}_i)$, the dipole S–matrix, (4.5) is nothing but the Balitsky–Kovchegov (BK) equation [19, 20] for the total S–matrix $Z_{ab} = S_{ab}$. The BFKL limit of the BK equation is obtained by defining the T–matrix $t = 1 - s$, $T = 1 - S$, and expanding T to linear order in t. One finds

$$\partial_Y T_Y(\boldsymbol{x}_{ab}) = \bar{\alpha}_s \int d^2\boldsymbol{x}_c\, K_{ab}(\boldsymbol{x}_c)\big[T_Y(\boldsymbol{x}_{ac}) + T_Y(\boldsymbol{x}_{cb}) - T_Y(\boldsymbol{x}_{ab})\big], \tag{4.6}$$

with

$$T_Y(\boldsymbol{x}_{ab}) = \int d^2\boldsymbol{x}_1 d^2\boldsymbol{x}_2\, t(\boldsymbol{x}_1,\boldsymbol{x}_2) n_Y(\boldsymbol{x}_{ab},\boldsymbol{x}_{12})\,. \tag{4.7}$$

Let us now turn to the timelike cascade and construct the probabilistic interpretation of the dipole evolution. First we recall the angular part of the real emission probability of k gluons in the soft kinematics [28],

$$d\mathcal{P}_k(p_a, p_1, \cdots p_k, p_b) = d^2\Omega_1 \cdots d^2\Omega_k \frac{1-\cos\theta_{ab}}{(1-\cos\theta_{a1})(1-\cos\theta_{12})\cdots(1-\cos\theta_{kb})}\,. \tag{4.8}$$

In the dipole language this can be viewed as the production probability of $(k+1)$–dipoles $(a,1),(1,2),\ldots,(k,b)$ obtained by multiplying together successive factors of the kernel K_{ij} according to a particular history of the dipole cascade. In the final result, the dependence on all the intermediately formed dipoles disappear and each factor in the denominator associates with one final dipole, while the numerator comes from the decay of the original dipole (a,b). Under the stereographic projection, (4.8) becomes

$$d\mathcal{P}_k(\boldsymbol{x}_a, \boldsymbol{x}_1, \cdots, \boldsymbol{x}_k \boldsymbol{x}_b) = d^2\boldsymbol{x}_1 \cdots d^2\boldsymbol{x}_k \frac{\boldsymbol{x}_{ab}^2}{\boldsymbol{x}_{a1}^2 \boldsymbol{x}_{12}^2 \cdots \boldsymbol{x}_{kb}^2}\,, \tag{4.9}$$

which is precisely the corresponding result for the spacelike cascade. Here the denominator contains a product of the squared length of each final dipole in the cascade, and the numerator contains the squared length of the original dipole.

One can similarly show that the virtual contributions are also mapped onto each other via the stereographic projection since they are simply obtained by integrating the real emission kernel K over final state coordinates. Therefore one is guaranteed to have the

[7] See [32] for an illuminating discussion on the consistency between (4.2) and (4.5).

exact timelike analog of the generating functional techniques described above. This is readily achieved by applying the stereographic projection to (4.1)

$$Z_{ab}[u,Y] = \sum_{n=1}^{\infty} \int \left(\prod_{i=1}^{n-1} \frac{d^2\Omega_i}{(1+\cos\theta_i)^2} \right) P_n(\boldsymbol{x}_1, \cdots \boldsymbol{x}_{n-1}; Y) u_1 u_2 \cdots u_n \,. \tag{4.10}$$

It is natural to define the probability distributions in the timelike case as

$$P_n(\Omega_1, \cdots, \Omega_{n-1}; Y) \equiv \frac{P_n(\boldsymbol{x}_1, \cdots, \boldsymbol{x}_{n-1}; Y)}{\prod_{i=1}^{n-1}(1+\cos\theta_i)^2} \,. \tag{4.11}$$

With this definition one can easily check that the evolution equations satisfied by P_n and Z_{ab} in the timelike case are identical in form to the corresponding equations (4.2) and (4.5) after replacing $\boldsymbol{x}_i \to \Omega_i$ everywhere.

For certain applications, mainly in the timelike context, the need arises to specify the energy (or rapidity) of individual partons. Equation (4.1) is not suitable for such purposes since $P_n(..., Y)$ is already integrated over energy. The more appropriate definition of the generating functional would be[8]

$$\tilde{Z}_{ab}[u,E] \equiv \sum_{n=1}^{\infty} \prod_{i=1}^{n} \left(\int d^2\boldsymbol{x}_i \int^E \frac{dk_i^0}{k_i^0} \right) \tilde{P}_n(\boldsymbol{x}_1, \cdots, \boldsymbol{x}_n) u_1 u_2 \cdots u_n \,, \tag{4.12}$$

where we have introduced the probability distribution of n gluons (rather than dipoles) which are ordered in energy, and accordingly, let the source function depend on one coordinate as well as on energy

$$u_i(\boldsymbol{x}_{i-1}, \boldsymbol{x}_i) \to u(\boldsymbol{x}_i, k_i^0) \,. \tag{4.13}$$

The equation for $\tilde{Z}$ is [21]

$$E\partial_E \tilde{Z}_{ab} = \bar{\alpha}_s \int d^2\boldsymbol{x}_c \, K_{ab}(\boldsymbol{x}_c)(-\tilde{Z}_{ab} + u(\boldsymbol{x}_c, E)\, \tilde{Z}_{ac}\, \tilde{Z}_{cb}) \,. \tag{4.14}$$

In the timelike case, the energy integral becomes $dk^0/k^0 = dY_s \to dY_t = dp^0/p^0$ and, due to the correspondence (4.8)–(4.9), it follows that $\prod_i d\boldsymbol{x}_i P_n(\{\boldsymbol{x}\}) \to \prod_i d\Omega_i P_n(\{\Omega\})$. Therefore, the equation for $\tilde{Z}$ in the timelike case is identical to (4.14) except that $\boldsymbol{x}_c$ is replaced by Ω_c.

The energy flow observable considered in [9] is the probability that the total amount of energy emitted into a specified interjet region $\mathcal{C}_{out}$ is less than $E_{out} \ll E$. The nonlinear evolution equation derived there has precisely the structure (4.14) with the weight function

$$u(\Omega_i, p_i^0) = \Theta_{in}(\Omega_i) + e^{-p_i^0/E_{out}} \Theta_{out}(\Omega_i) \,. \tag{4.15}$$

This follows from the kinematical constraint

$$\Theta(E_{out} - \sum_{j \in \mathcal{C}_{out}} p_j^0) \approx \prod_{i=1}^{n-1} \left(\Theta_{in}(\Omega_i) + e^{-p_i^0/E_{out}} \Theta_{out}(\Omega_i) \right) \,, \tag{4.16}$$

[8] In fact, this was the original definition employed in [21].

where $\Theta_{out}(\Omega)$ is the support function nonvanishing in $\mathcal{C}_{out}$ and $\Theta_{in}(\Omega) \equiv 1 - \Theta_{out}(\Omega)$.

More generally, for each physically motivated choice of $u(\Omega_i, p_i^\mu)$ or $u(\Omega_{i-1}, \Omega_i)$ ($u(\boldsymbol{x}_i, k_i^\mu)$ or $u(\boldsymbol{x}_{i-1}, \boldsymbol{x}_i)$ in the spacelike case) the generating functional becomes an observable. Although the interpretations of the resulting evolution equations (with or without a u–factor in the nonlinear term) vary drastically depending on the context, mathematically they are equivalent and can be mapped to one another via the stereographic projection.

5. Dipole pair density

Having established the timelike version of Mueller's dipole model, we can now in principle study arbitrary higher order correlations among dipoles in the interjet region of e^+e^- annihilation. Physically this is relevant to the number correlation of heavy–quark pairs. Similarly to the single dipole distribution $n_Y(\boldsymbol{x}_{ab}, \boldsymbol{x}_{cd})$ (4.3), one can define the k–dipole inclusive distribution by differentiating k times the generating functional

$$n_Y^{(k)}(\boldsymbol{x}_{ab}; \boldsymbol{x}_{11'}, \boldsymbol{x}_{22'}, ..., \boldsymbol{x}_{kk'}) = \frac{1}{k!} \left. \frac{\delta^k Z_{ab}}{\delta u(\boldsymbol{x}_1, \boldsymbol{x}_{1'}) \delta u(\boldsymbol{x}_2, \boldsymbol{x}_{2'}) ... \delta u(\boldsymbol{x}_k, \boldsymbol{x}_{k'})} \right|_{u=1} . \tag{5.1}$$

The corresponding distribution in the timelike case can be immediately inferred from (4.11). In the case of $k = 2$ ('the dipole pair density' [29]), we find

$$n_Y^{(2)}(\Omega_{ab}, \Omega_{11'}, \Omega_{22'}) = \frac{1}{\prod_{i=11'22'} (1 + \cos\theta_i)^2} \, n_Y^{(2)}(\boldsymbol{x}_{ab}, \boldsymbol{x}_{11'}, \boldsymbol{x}_{22'}) \, . \tag{5.2}$$

In [33], an exact integral representation of $n_Y^{(2)}(\boldsymbol{x}_{ab}, \boldsymbol{x}_{11'}, \boldsymbol{x}_{22'})$ has been derived. [See also [34].] Unfortunately, the expression is too complicated to be evaluated in full generality. However, in certain limits analytical results are available [23, 24]. These include the large parent limit

$$|\boldsymbol{x}_{ab}| \gg |\boldsymbol{x}_{12}| \gg |\boldsymbol{x}_{11'}|, |\boldsymbol{x}_{22'}| \, , \tag{5.3}$$

and the small parent limit

$$|\boldsymbol{x}_{a1}|, |\boldsymbol{x}_{a2}|, |\boldsymbol{x}_{12}| \gg |\boldsymbol{x}_{ab}|, |\boldsymbol{x}_{11'}|, |\boldsymbol{x}_{22'}| \, . \tag{5.4}$$

As observed in [23], the above two configurations are transformed to each other via a conformal transformation. This means that the results can be unified in a single expression which involves anharmonic ratios

$$n_Y^{(2)}(\boldsymbol{x}_{ab}, \boldsymbol{x}_{11'}, \boldsymbol{x}_{22'}) \sim \frac{e^{2\chi(\gamma_s')Y}}{\boldsymbol{x}_{11'}^4 \boldsymbol{x}_{22'}^4} \left(\frac{\boldsymbol{x}_{11'}^2 \boldsymbol{x}_{22'}^2}{\boldsymbol{x}_{12}^4} \right)^{1-\gamma_s'} \left(\frac{\boldsymbol{x}_{ab}^2 \boldsymbol{x}_{12}^2}{\boldsymbol{x}_{a1}^2 \boldsymbol{x}_{b2}^2} \right)^{1-\gamma_s} , \tag{5.5}$$

where the anomalous dimensions $0 < \gamma_s < \gamma_s' < 1/2$ are determined from certain saddle point conditions.[9] Using (5.2), (5.5) and the stereographic projection, we find

$$n_Y^{(2)}(\Omega_{ab}, \Omega_{11'}, \Omega_{22'}) \sim \frac{e^{2\chi(\gamma_s')Y}}{(1 - \cos\theta_{11'})^2 (1 - \cos\theta_{22'})^2} \left(\frac{(1 - \cos\theta_{11'})(1 - \cos\theta_{22'})}{(1 - \cos\theta_{12})^2} \right)^{1-\gamma_s'} \times \left(\frac{(1 - \cos\theta_{ab})(1 - \cos\theta_{12})}{(1 - \cos\theta_{a1})(1 - \cos\theta_{b2})} \right)^{1-\gamma_s} \tag{5.6}$$

[9] See [23] for details. Our normalization of $n^{(2)}$ differs from that in [23] by a factor $(\boldsymbol{x}_{11'}^2 \boldsymbol{x}_{22'}^2)^{-1}$. Also the anomalous dimension is redefined as $\gamma \to 1 - \gamma$.

The case (5.3) includes the back–to–back configuration $\theta_{ab} = \pi$. [See fig. 2, but this time the gluons 1 and 2 are replaced by the dipoles 11' and 22'.] The expression in (5.6) then reduces to

$$n_Y^{(2)}(\Omega_{ab}, \Omega_{11'}, \Omega_{22'}) \sim \frac{e^{2\chi(\gamma_s')Y}}{\theta_{11'}^{2+2\gamma_s'}\theta_{22'}^{2+2\gamma_s'}} \frac{1}{(1-\cos\theta_{12})^{1-2\gamma_s'+\gamma_s}} \times \frac{1}{(1-\cos\theta_{a1})^{1-\gamma_s}(1-\cos\theta_{b2})^{1-\gamma_s}}\,, \tag{5.7}$$

where the result is valid when $2(1-\cos\theta_{12}) \ll (1-\cos\theta_{a1})(1-\cos\theta_{b2})$. On the other hand, the case (5.4) corresponds to radiation from a highly boosted $q\bar{q}$ jets such that $\theta_{ab} \ll 1$. Equation (5.6) then reduces to

$$n_Y^{(2)}(\Omega_{ab}, \Omega_{11'}, \Omega_{22'}) \sim \frac{e^{2\chi(\gamma_s')Y}}{\theta_{11'}^{2+2\gamma_s'}\theta_{22'}^{2+2\gamma_s'}} \frac{1}{(1-\cos\theta_{12})^{1-2\gamma_s'+\gamma_s}} \times \frac{\theta_{ab}^{2-2\gamma_s}}{(1-\cos\theta_{a1})^{1-\gamma_s}(1-\cos\theta_{a2})^{1-\gamma_s}}\,. \tag{5.8}$$

It is interesting to compare (5.7) and (5.8) with the two–gluon correlation function (3.18), (3.21). Putting aside a possible numerical difference in γ_s, we see that the growth of the correlation as $\theta_{12} \to 0$ in (5.8) is significantly weaker than in (3.18). This is of course due to the color screening effect of dipoles. Moreover, when θ_{12} becomes comparable to either $\theta_{11'}$ or $\theta_{22'}$ the correlation function converges to a finite value. This conclusion cannot be reached from (5.6) which assumes $\theta_{12} \gg \theta_{11'}, \theta_{22'}$. Rather, it follows from a proper evaluation of $n_Y^{(2)}$ in the regime $\theta_{12} \approx \theta_{11'}, \theta_{22'}$ (or $|\boldsymbol{x}_{12}| \approx |\boldsymbol{x}_{11'}|, |\boldsymbol{x}_{22'}|$) as was done in [24]. [In the spacelike case this regime deserves special attention in association with the BK equation.]

6. Energy correlation function

In [25], the small angle limit of the energy–energy correlation functions in e^+e^- annihilation was studied using the method of the operator product expansion (OPE)

$$\langle \mathcal{E}(\Omega_1)\mathcal{E}(\Omega_2)\rangle \sim \frac{1}{|\theta_{12}|^{2+2\gamma(3)}}\,, \quad (\theta_{12} \to 0)\,, \tag{6.1}$$

where $\gamma(j)$ is the anomalous dimension of the twist–two operators with spin j. Essentially the same OPE applies to the high energy hadron problem [22]

$$\langle \mathcal{E}(\boldsymbol{x}_1)\mathcal{E}(\boldsymbol{x}_2)\rangle \sim \frac{1}{|\boldsymbol{x}_{12}|^{2+2\gamma(3)}}\,, \quad (\boldsymbol{x}_{12} \to 0)\,. \tag{6.2}$$

It is straightforward to generalize these results to higher point correlation functions

$$\langle \mathcal{E}(\Omega_1)\mathcal{E}(\Omega_2)\cdots\mathcal{E}(\Omega_k)\rangle \sim \frac{1}{\theta^{2k-2+2\gamma(k+1)}}\,, \tag{6.3}$$

and

$$\langle \mathcal{E}(\boldsymbol{x}_1)\mathcal{E}(\boldsymbol{x}_2)\cdots\mathcal{E}(\boldsymbol{x}_k)\rangle \sim \frac{1}{|\boldsymbol{x}|^{2k-2+2\gamma(k+1)}}\,, \tag{6.4}$$

where we let the relative angles θ_{ij} and coordinates $|\boldsymbol{x}_i - \boldsymbol{x}_j|$ all go to zero while keeping their ratios fixed, and denoted their representative values by θ and $\boldsymbol{x}$, respectively.

The above results are valid not only in $\mathcal{N} = 4$ SYM where they were originally derived [25], but also in any conformal theory. In QCD, they are expected to hold in approximations where the running of the coupling is neglected (as in the leading order BFKL). In this section we study the energy correlation functions in the dipole model and provide a concrete physical picture of how these singular behaviors are dynamically generated in the parton evolution. While there is the usual caveat about discussing energy–related observables in energy–nonconserving approximations, we believe that the dominant configuration which we shall identify below continues to be the relevant one even after a proper implementation of energy conservation both in the timelike [35] and spacelike [36] gluon cascades.

6.1 The energy two–point function

We first consider the energy two–point function. Though the primary interest in the correlation functions arises in the context of e^+e^- annihilation where they are experimentally measurable, we find that the actual calculations are a little more transparent in the $\boldsymbol{x}$–space.[10] Of course, via the stereographic projection all the equations to follow have a timelike counterpart. We employ the energy ordering scheme and write $Y = \ln(E/k^0)$. The energy two-point function can be generically written as

$$\begin{aligned}\langle \mathcal{E}(\boldsymbol{x}_1)\mathcal{E}(\boldsymbol{x}_2)\rangle &= \int_0^\infty dY_2 \int_0^\infty dY_1\, k_1^0 k_2^0\, n(\boldsymbol{x}_1, Y_1, \boldsymbol{x}_2, Y_2) \\ &= 2E^2 \int_0^\infty dY_2\, e^{-Y_2} \int_0^{Y_2} dY_1\, e^{-Y_1} n(\boldsymbol{x}_1, Y_1, \boldsymbol{x}_2, Y_2)\,,\end{aligned} \tag{6.5}$$

where $n(x_1, Y_1, \boldsymbol{x}_2, Y_2)$ is the number density of gluon pairs with rapidities Y_1 and Y_2 located at $\boldsymbol{x}_1$ and $\boldsymbol{x}_2$, respectively. At high energy, we would like to relate this quantity to the single dipole density $n_Y(\boldsymbol{x}_{ab}, \boldsymbol{x}_{12})$. [Henceforth we suppress the dependence on the parent dipole coordinates $\boldsymbol{x}_{ab}$ in n_Y and set $|\boldsymbol{x}_{ab}| = 1$.]

In general, there is no universal relation between $n(\boldsymbol{x}_1, Y_1, \boldsymbol{x}_2, Y_2)$ and $n_Y(\boldsymbol{x}_{12})$; the former carries information on the rapidity of the gluons 1 and 2 (in a cascaded evolved up to $Y \to \infty$), whereas the latter simply counts the total number of dipoles $(\boldsymbol{x}_1, \boldsymbol{x}_2)$ in a cascade evolved up to Y without specifying the energy of their constituents. However, as long as the singular behavior in the limit $\boldsymbol{x}_1 \to \boldsymbol{x}_2$ is concerned, the two quantities can be linked by the following argument: For a given gluon pair with rapidities Y_1 and Y_2 such that $Y_2 > Y_1$, the strongest correlation comes from the moment in the history of the cascade when the two gluons in question were realized as a dipole as a result of the emission of the gluon with rapidity Y_2. The number of such pairs at the time of creation

[10] The schematic argument given in [22] overlooks the subtleties to be raised in the following. Our refined argument is physically more correct and readily generalizes to higher order correlation functions.

is related to $\partial_{Y_2} n_{Y_2}(\boldsymbol{x}_{12})$ where the derivative is because the gluon 2 has rapidity exactly equal to Y_2 (rather than integrated over rapidity). This is, however, still inclusive in the rapidity of the gluon 1. Therefore, we are led to define the "unintegrated" dipole density, $n^u(\boldsymbol{x}_1, Y_1, \boldsymbol{x}_2, Y_2)$, as follows

$$\partial_{Y_2} n_{Y_2}(\boldsymbol{x}_{12}) = \int_0^{Y_2} dY_1\, n^u(\boldsymbol{x}_1, Y_1, \boldsymbol{x}_2, Y_2)\,. \tag{6.6}$$

To proceed, we observe that n^u is approximately independent of Y_2. In order to see this, consider a simple toy model of the dipole cascade in which we neglect the transverse dimensions and assume each dipole to split after a fixed rapidity interval[11] ΔY. At $Y = 0$, there is only one dipole composed of a quark and an antiquark both having $Y = 0$ which we denote as $(0, 0)$. This dipole emits a gluon at rapidity ΔY and splits into two dipoles $(0, \Delta Y)$ and $(\Delta Y, 0)$. In the second step these two child dipoles split into four dipoles $(0, 2\Delta Y)$, $(2\Delta Y, \Delta Y)$, $(\Delta Y, 2\Delta Y)$ and $(2\Delta Y, 0)$. The process stops after $n = Y_{tot}/\Delta Y$ steps, with Y_{tot} being the total rapidity, and generates $2^n = 2^{Y_{tot}/\Delta Y} = \exp\{(\ln 2/\Delta Y) Y_{tot}\}$ dipoles. One can easily see that there are $2^{(Y/\Delta Y)-1}$ gluons having rapidity Y. In particular, half of the total number of gluons have the maximal value $Y = Y_{tot}$. This means that all the dipoles have the rapidity composition either (Y_{tot}, Y) or (Y, Y_{tot}) and their number depends only on Y, and not on Y_{tot}. In the full model the rapidity distribution is more smeared out than in the toy model, but it will again be true that the density $n^u(\boldsymbol{x}_1, Y_1, \boldsymbol{x}_2, Y_2)$ is largely determined by the gluons at Y_1, since their number is exponentially smaller than the number of gluons at Y_2 in the presence of the strong energy ordering $Y_2 \gg Y_1$.

We thus write $n^u = n^u(\boldsymbol{x}_1, \boldsymbol{x}_2, Y_1)$ and get

$$\partial^2_{Y_1} n_{Y_1}(\boldsymbol{x}_{12}) = n^u(\boldsymbol{x}_1, \boldsymbol{x}_2, Y_1)\,, \tag{6.8}$$

as the number density of dipoles $(\boldsymbol{x}_1, \boldsymbol{x}_2)$ having the rapidity composition (Y_1, Y_2) in a cascade evolved up to Y_2. Later in the evolution (i.e., at $Y > Y_2$) these dipoles may or may not split, but the gluons 1 and 2 remain fixed at their original positions $(\boldsymbol{x}_1, \boldsymbol{x}_2)$. Since the total probability of all the decay channels is unity, the most singular contribution (as $\boldsymbol{x}_{12} \to 0$) to the two–gluon distribution $n(\boldsymbol{x}_1, Y_1, \boldsymbol{x}_2, Y_2)$ in (6.5) which is in principle defined in a cascade evolved up to $Y = \infty$ is actually frozen at $Y = Y_2$ (or at whatever value $Y > Y_1$) and is given by (6.8).

We now recall the integral expression (3.10) for $n_Y(\boldsymbol{x}_{12})$ in the limit $\boldsymbol{x}_{12} \to 0$

$$n_Y(\boldsymbol{x}_{12}) = \frac{1}{\boldsymbol{x}_{12}^2} \int \frac{dj}{2\pi i} c(j) \frac{e^{(j-1)Y}}{|\boldsymbol{x}_{12}|^{2\gamma(j)}}\,, \tag{6.9}$$

where the contour j–integral goes around the branch cut in the Jacobian $c(j)$

$$c(j) \propto \frac{\partial \gamma(j)}{\partial j} \approx \frac{-1}{2\sqrt{14\bar{\alpha}_s \zeta(3)(j - j_0)}}\,. \quad (j_0 = 1 + 4\bar{\alpha}_s \ln 2) \tag{6.10}$$

[11] In the full model one has

$$\Delta Y \sim \frac{1}{\bar{\alpha}_s \ln(\boldsymbol{x}_{ab}^2/\rho^2)}\,, \tag{6.7}$$

where ρ is a small cutoff.

Using this, we find the energy–energy correlator

$$\begin{aligned}\langle \mathcal{E}(\boldsymbol{x}_1)\mathcal{E}(\boldsymbol{x}_2)\rangle &\approx 2E^2\int_0^\infty dY_2 e^{-Y_2}\int_0^{Y_2} dY_1 e^{-Y_1}\partial_{Y_1}^2 n_{Y_1}(\boldsymbol{x}_{12})\\ &= 2E^2\frac{1}{\boldsymbol{x}_{12}^2}\int\frac{dj}{2\pi i}c(j)\frac{(j-1)^2}{3-j}\frac{1}{|\boldsymbol{x}_{12}|^{2\gamma(j)}}\,.\end{aligned} \tag{6.11}$$

Deforming the contour and picking up the pole at $j=3$, we find

$$\langle \mathcal{E}(\boldsymbol{x}_1)\mathcal{E}(\boldsymbol{x}_2)\rangle \sim \frac{E^2}{|\boldsymbol{x}_{12}|^{2+2\gamma(3)}}+\frac{1}{\boldsymbol{x}_{12}^2}\int_{Rej>3} dj\cdots\frac{1}{|\boldsymbol{x}_{12}|^{2\gamma(j)}}\,. \tag{6.12}$$

Since $\gamma(j)<\gamma(3)$ for $j>3$, the contribution from the second term is subdominant in the limit $\boldsymbol{x}_{12}\to 0$. We therefore recover the OPE result (6.2).

6.2 The energy three–point function and beyond

The energy three–point function is given by

$$\langle \mathcal{E}(\boldsymbol{x}_1)\mathcal{E}(\boldsymbol{x}_2)\mathcal{E}(\boldsymbol{x}_3)\rangle = 3!E^3\int_0^\infty dY_3 e^{-Y_3}\int_0^{Y_3} dY_2 e^{-Y_2}\int_0^{Y_2} dY_1 e^{-Y_1} n(\boldsymbol{x}_1,Y_1,\boldsymbol{x}_2,Y_2,\boldsymbol{x}_3,Y_3)\,, \tag{6.13}$$

where we $n(...,\boldsymbol{x}_3,Y_3)$ is the distribution function of three gluons. The leading singular behavior as $\boldsymbol{x}_{ij}\to 0$ arises from the configuration where the three gluons are realized as two contiguous dipoles which, for $Y_3>Y_2>Y_1$, are $(\boldsymbol{x}_1,\boldsymbol{x}_3)$ and $(\boldsymbol{x}_3,\boldsymbol{x}_2)$. This occurs when the gluon 3 is emitted from dipoles $(\boldsymbol{x}_1,\boldsymbol{x}_2)$ whose number density is given by (6.8). Thus to get the number density of the dipole pairs $(\boldsymbol{x}_1,\boldsymbol{x}_3)$ and $(\boldsymbol{x}_3,\boldsymbol{x}_2)$ with rapidity composition (Y_1,Y_3) and (Y_3,Y_2), we just need to multiply (6.8) by the emission probability. This gives the unintegrated density

$$n^u(\boldsymbol{x}_1,Y_1,\boldsymbol{x}_2,Y_2,\boldsymbol{x}_3,Y_3)\approx\bar{\alpha}_s K_{12}(\boldsymbol{x}_3)\partial_{Y_1}^2 n_{Y_1}(\boldsymbol{x}_{12})\,. \tag{6.14}$$

We now substitute this quantity in (6.13) as a dipole model analog of the three gluon distribution. We remind the reader that this is justified only for the singular contribution in the limit $\boldsymbol{x}_{ij}\to 0$. Writing $\boldsymbol{x}_{ij}\sim\boldsymbol{x}$ and therefore $K_{12}(\boldsymbol{x}_3)\sim\frac{1}{\boldsymbol{x}^2}$, (6.13) then becomes

$$\begin{aligned}\langle \mathcal{E}(\boldsymbol{x}_1)\mathcal{E}(\boldsymbol{x}_2)\mathcal{E}(\boldsymbol{x}_3)\rangle &\sim E^3\int_0^\infty dY_3 e^{-Y_3}\int_0^{Y_3} dY_2 e^{-Y_2}\int_0^{Y_2} dY_1 e^{-Y_1}\\ &\quad\times\frac{\bar{\alpha}_s}{\boldsymbol{x}^4}\int\frac{dj}{2\pi i}c(j)(j-1)^2 e^{(j-1)Y_1}\left(\frac{1}{\boldsymbol{x}}\right)^{2\gamma(j)}\\ &= \frac{\bar{\alpha}_s E^3}{\boldsymbol{x}^4}\int\frac{dj}{2\pi i}c(j)\frac{(j-1)^2}{2(4-j)}\frac{1}{|\boldsymbol{x}|^{2\gamma(j)}}\\ &\sim \bar{\alpha}_s E^3\frac{1}{|\boldsymbol{x}|^{4+2\gamma(4)}}\,,\end{aligned} \tag{6.15}$$

in agreement with (6.4).

It is now straightforward to extend the above result to the energy k–point correlation function

$$\langle \mathcal{E}(\boldsymbol{x}_1)\mathcal{E}(\boldsymbol{x}_2)\cdots\mathcal{E}(\boldsymbol{x}_k)\rangle = k!E^k \int_0^\infty dY_k e^{-Y_k}\cdots\int_0^{Y_2} dY_1 e^{-Y_1} n(\boldsymbol{x}_1,Y_1,\boldsymbol{x}_2,Y_2,\ldots,\boldsymbol{x}_k,Y_k)\,. \tag{6.16}$$

The leading singular contribution to the k–gluon distribution $n(...,\boldsymbol{x}_k,Y_k)$ with $Y_k > Y_{k-1} > \cdots > Y_1$ comes from the process where we start with the lowest rapidity pair $(\boldsymbol{x}_1,\boldsymbol{x}_2)$ and successively emit the remaining gluons, creating first the pair $(\boldsymbol{x}_1,\boldsymbol{x}_3)$ and $(\boldsymbol{x}_3,\boldsymbol{x}_2)$, then emitting the gluon 4 from either of these two dipoles, and so on. One then gets the fully unintegrated distribution[12]

$$\bar\alpha_s^{k-2} K_{12}(\boldsymbol{x}_3)K_{32}(\boldsymbol{x}_4)\cdots K_{k-1,2}(\boldsymbol{x}_k)\,\partial^2_{Y_1} n_{Y_1}(\boldsymbol{x}_{12}) \sim \left(\frac{\bar\alpha_s}{\boldsymbol{x}^2}\right)^{k-2}\partial^2_{Y_1} n_{Y_1}(\boldsymbol{x}_{12})\,. \tag{6.17}$$

Substituting this in (6.16) as a proxy for the k–gluon distribution $n(...,\boldsymbol{x}_k,Y_k)$, one finds the result

$$\begin{aligned}\langle \mathcal{E}(\boldsymbol{x}_1)\mathcal{E}(\boldsymbol{x}_2)\cdots\mathcal{E}(\boldsymbol{x}_k)\rangle &\sim \bar\alpha_s^{k-2}E^k\frac{1}{\boldsymbol{x}^{2(k-2)}}\int_0^\infty dY_k e^{-Y_k}\cdots\int_0^{Y_2} dY_1 e^{-Y_1}\\ &\quad\times\frac{1}{\boldsymbol{x}^2}\int\frac{dj}{2\pi i}c(j)(j-1)^2\,e^{(j-1)Y_1}\frac{1}{|\boldsymbol{x}|^{2\gamma(j)}}\\ &\sim E^k\bar\alpha_s^{k-2}\frac{1}{|\boldsymbol{x}|^{2\gamma(k+1)+2k-2}}\,.\end{aligned} \tag{6.18}$$

Summarizing, in the dipole picture the most singular contribution to the k–point energy correlation function comes from the moment in the history of the dipole cascade when the k gluons are realized as a single chain of $k-1$ dipoles. This chain represents successive emissions of energy ordered gluons at comparable separations (collinear emissions at comparable angles in the timelike case). Later in the evolution the chain decays, but the k gluons remain in their original positions. Integrating over all possible values of rapidity at which this chain is formed, one recovers the OPE result.

In strongly coupled $\mathcal{N}=4$ SYM the AdS/CFT correspondence allows one to represent the energy correlation function as the scattering amplitude between the photon (the primary $q\bar q$ pair) and the graviton (energy operator insertions, or calorimeters) [25]. Its small angle limit is associated with the Regge behavior of the string S–matrix and is dominated by the t–channel exchange of a massive string state ('Pomeron') with an anomalous dimension $\gamma(1+k)$. A similar interpretation is possible in QCD by identifying the t–channel object with the BFKL Pomeron. Naively, one may expect from the relevant configurations that the k–point function would be related to the $(k-1)$–ple dipole density $n_Y^{(k-1)}$ (cf. (5.1)) which involves the exchange of $(k-1)$ Pomerons with an anomalous dimension $\gamma=\chi^{-1}(4(k-1)\ln 2)$ [37]. However, specifying the rapidity of k gluons amounts to taking the k–th derivative of $n_Y^{(k-1)}$ with respect to Y. Each Y–derivative lowers the degree of

[12]This expression is valid for a particular color ordering of the dipoles, but since in the end we let all $|\boldsymbol{x}_i-\boldsymbol{x}_j|$ go to zero with fixed ratios, the result holds for any ordering.

multiplicity, thus one has a cascade of distributions $n^{(k-1)} \to n^{(k-2)} \to n^{(k-3)} \to \cdots$ [38]. The fully unintegrated distribution obtained in this way involves the single dipole density or the single Pomeron exchange with an unusual value of the anomalous dimension $\gamma(1+k)$.

Acknowledgements

The work of Y. H. and T. M. is supported, in part, by Special Coordination Funds for Promoting Science and Technology of the Ministry of Education, Culture, Sports, Science and Technology, the Japanese Government.

A. Next-to-leading order dipole kernel in e^+e^-–annihilation

Recently, Balitsky and Chirilli have derived the spacelike next–to–leading logarithmic (NLL) dipole kernel in $\mathcal{N} = 4$ SYM which turned out to be conformally (Möbius) symmetric [27] (see, also, [39]). As we noted in Section 2, in this theory there is a rather strong indication that the stereographic projection works to all orders of the soft approximation. Assuming this to be correct, one can immediately obtain from their result the NLL kernel for the dipole evolution in the timelike case by applying the stereographic projection. The evolution equation for the dipole density which generalizes the leading order equation (4.4) is

$$\begin{aligned}\partial_Y n_Y(\Omega_{ab}) \,=\, \bar{\alpha}_s \left(1 - \bar{\alpha}_s \frac{\pi^2}{12}\right) \int d^2\Omega_c \, K_{ab}(\Omega_c) \big[n_Y(\Omega_{ac}) + n_Y(\Omega_{cb}) - n_Y(\Omega_{ab})\big] \\ + \bar{\alpha}_s^2 \int d^2\Omega_c d^2\Omega_d K'_{ab}(\Omega_c, \Omega_d) n_Y(\Omega_{cd}) \,, \end{aligned} \tag{A.1}$$

where

$$\begin{aligned} K'_{ab}(\Omega_c, \Omega_d) \,=\, \frac{1}{8\pi^2} \Bigg\{ & \frac{(1-\cos\theta_{ab})}{(1-\cos\theta_{ac})(1-\cos\theta_{cd})(1-\cos\theta_{db})} \\ & \times \Bigg[\left(1 + \frac{(1-\cos\theta_{ab})(1-\cos\theta_{cd})}{(1-\cos\theta_{ac})(1-\cos\theta_{bd}) - (1-\cos\theta_{ad})(1-\cos\theta_{bc})}\right) \\ & \times \ln \frac{(1-\cos\theta_{ac})(1-\cos\theta_{bd})}{(1-\cos\theta_{ad})(1-\cos\theta_{bc})} + 2 \ln \frac{(1-\cos\theta_{ab})(1-\cos\theta_{cd})}{(1-\cos\theta_{ad})(1-\cos\theta_{bc})} \Bigg] \\ & + \, 12\pi^2 \zeta(3) \delta^{(2)}(\Omega_{ac}) \delta^{(2)}(\Omega_{bd}) \Bigg\} . \end{aligned} \tag{A.2}$$

The eigenfunctions and the eigenvalues can be exactly mapped as well.

B. The correspondence between boost and dilatation

The correspondence of the gluon distribution has an interesting property under boost. One can see from (2.5) that the dilatation in the x–coordinates,

$$x^\mu \to x'^\mu = \lambda x^\mu \tag{B.1}$$

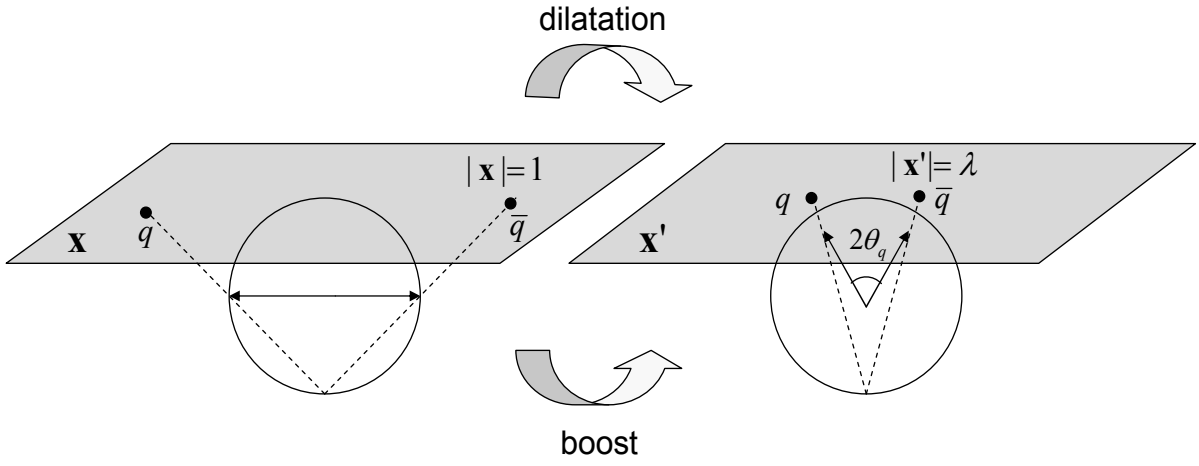

Figure 5: *Boosting the $q\bar{q}$ pair in e^+e^- annihilation corresponds to changing the size of the dipole in high energy scattering.*

translates into the boost in the y^3 direction

$$y^+ = \lambda y'^+, \quad y^- = \frac{y'^-}{\lambda}, \quad \boldsymbol{y} = \boldsymbol{y}' \,. \tag{B.2}$$

This transformation relates the gluon distribution in the boosted frame to that generated by a squeezed dipole. For simplicity, assume that the initial quark–antiquark pair is oriented to the y^1–axis (see fig. 5). λ is related to the velocity v of the boost via

$$\lambda = \frac{1}{\gamma(1+v)} \,, \tag{B.3}$$

where $\gamma = 1/\sqrt{1-v^2}$ as usual. Since $v = \cos\theta_q$ in the new frame where θ_q is the angle of the quark jet, one has

$$\lambda = \frac{1}{\gamma(1+v)} = \frac{\sin\theta_q}{1+\cos\theta_q} = |\boldsymbol{x}| \,, \tag{B.4}$$

consistently with (B.1).

Under the dilatation (B.1), the energy distribution (2.6) transforms as

$$\mathcal{E}'(\boldsymbol{x}') = \frac{1}{\lambda^3}\mathcal{E}(\boldsymbol{x}) \tag{B.5}$$

The distribution in the boosted frame is

$$\mathcal{E}(\Omega') = \frac{2}{(1+\cos\theta')^3}\mathcal{E}(\boldsymbol{x}') = \frac{1}{\lambda^3}\frac{(1+\cos\theta)^3}{(1+\cos\theta')^3}\mathcal{E}(\Omega) \tag{B.6}$$

Using the relation

$$\cos\theta' = \frac{v+\cos\theta}{1+v\cos\theta} \tag{B.7}$$

one finds

$$\mathcal{E}(\Omega') = \frac{1}{\gamma^3(1 - v\cos\theta')^3}\mathcal{E}[\Omega(\Omega')] \tag{B.8}$$

Similarly the number (or the charge) distribution transforms as

$$\frac{dN}{d\Omega'} = \frac{1}{\gamma^2(1 - v\cos\theta')^2}\frac{dN[\Omega(\Omega')]}{d\Omega} \tag{B.9}$$

References

[1] S. Kluth, "Tests of quantum chromo dynamics at e+ e- colliders," *Rept. Prog. Phys.* **69** (2006) 1771–1846, hep-ex/0603011.

[2] N. A. Sveshnikov and F. V. Tkachov, "Jets and quantum field theory," *Phys. Lett.* **B382** (1996) 403–408, hep-ph/9512370.

[3] G. P. Korchemsky, G. Oderda, and G. Sterman, "Power corrections and nonlocal operators," hep-ph/9708346.

[4] G. Oderda and G. Sterman, "Energy and color flow in dijet rapidity gaps," *Phys. Rev. Lett.* **81** (1998) 3591–3594, hep-ph/9806530.

[5] A. V. Belitsky, G. P. Korchemsky, and G. Sterman, "Energy flow in QCD and event shape functions," *Phys. Lett.* **B515** (2001) 297–307, hep-ph/0106308.

[6] C. F. Berger, T. Kucs, and G. Sterman, "Energy flow in interjet radiation," *Phys. Rev.* **D65** (2002) 094031, hep-ph/0110004.

[7] M. Dasgupta and G. P. Salam, "Resummation of non-global QCD observables," *Phys. Lett.* **B512** (2001) 323–330, hep-ph/0104277.

[8] M. Dasgupta and G. P. Salam, "Accounting for coherence in interjet E(t) flow: A case study," *JHEP* **03** (2002) 017, hep-ph/0203009.

[9] A. Banfi, G. Marchesini, and G. Smye, "Away-from-jet energy flow," *JHEP* **08** (2002) 006, hep-ph/0206076.

[10] Y. L. Dokshitzer and G. Marchesini, "On large angle multiple gluon radiation," *JHEP* **03** (2003) 040, hep-ph/0303101.

[11] C. F. Berger, T. Kucs, and G. Sterman, "Event shape / energy flow correlations," *Phys. Rev.* **D68** (2003) 014012, hep-ph/0303051.

[12] G. Marchesini and E. Onofri, "Exact solution of BFKL equation in jet-physics," *JHEP* **07** (2004) 031, hep-ph/0404242.

[13] J. R. Forshaw, A. Kyrieleis, and M. H. Seymour, "Gaps between jets in the high energy limit," *JHEP* **06** (2005) 034, hep-ph/0502086.

[14] J. R. Forshaw, A. Kyrieleis, and M. H. Seymour, "Super-leading logarithms in non-global observables in QCD," *JHEP* **08** (2006) 059, hep-ph/0604094.

[15] A. Banfi, G. Corcella, and M. Dasgupta, "Angular ordering and parton showers for non-global QCD observables," *JHEP* **03** (2007) 050, hep-ph/0612282.

[16] G. Marchesini and A. H. Mueller, "BFKL dynamics in jet evolution," *Phys. Lett.* **B575** (2003) 37–44, hep-ph/0308284.

[17] E. A. Kuraev, L. N. Lipatov, and V. S. Fadin, "The Pomeranchuk Singularity in Nonabelian Gauge Theories," *Sov. Phys. JETP* **45** (1977) 199–204.

[18] I. I. Balitsky and L. N. Lipatov, "The Pomeranchuk Singularity in Quantum Chromodynamics," *Sov. J. Nucl. Phys.* **28** (1978) 822–829.

[19] I. Balitsky, "Operator expansion for high-energy scattering," *Nucl. Phys.* **B463** (1996) 99–160, hep-ph/9509348.

[20] Y. V. Kovchegov, "Small-x F2 structure function of a nucleus including multiple pomeron exchanges," *Phys. Rev.* **D60** (1999) 034008, hep-ph/9901281.

[21] A. H. Mueller, "Soft gluons in the infinite momentum wave function and the BFKL pomeron," *Nucl. Phys.* **B415** (1994) 373–385.

[22] Y. Hatta, "Relating e^+e^- annihilation to high energy scattering at weak and strong coupling," *JHEP* **11** (2008) 057, 0810.0889.

[23] Y. Hatta and A. H. Mueller, "Correlation of small-x gluons in impact parameter space," *Nucl. Phys.* **A789** (2007) 285–297, hep-ph/0702023.

[24] E. Avsar and Y. Hatta, "Quantitative study of the transverse correlation of soft gluons in high energy QCD," *JHEP* **09** (2008) 102, 0805.0710.

[25] D. M. Hofman and J. Maldacena, "Conformal collider physics: Energy and charge correlations," *JHEP* **05** (2008) 012, 0803.1467.

[26] L. Cornalba, "Eikonal Methods in AdS/CFT: Regge Theory and Multi-Reggeon Exchange," 0710.5480.

[27] I. Balitsky and G. A. Chirilli, "Conformal kernel for NLO BFKL equation in $\mathcal{N}$=4 SYM," 0812.3416.

[28] A. Bassetto, M. Ciafaloni, and G. Marchesini, "Jet Structure and Infrared Sensitive Quantities in Perturbative QCD," *Phys. Rept.* **100** (1983) 201–272.

[29] A. H. Mueller, "Unitarity and the BFKL pomeron," *Nucl. Phys.* **B437** (1995) 107–126, hep-ph/9408245.

[30] L. N. Lipatov, "Small-x physics in perturbative QCD," *Phys. Rept.* **286** (1997) 131–198, hep-ph/9610276.

[31] H. Navelet and R. B. Peschanski, "Conformal invariance and the exact solution of BFKL equations," *Nucl. Phys.* **B507** (1997) 353–366, hep-ph/9703238.

[32] E. Levin and M. Lublinsky, "A linear evolution for non-linear dynamics and correlations in realistic nuclei," *Nucl. Phys.* **A730** (2004) 191–211, hep-ph/0308279.

[33] R. B. Peschanski, "Dual Shapiro-Virasoro amplitudes in the QCD dipole picture," *Phys. Lett.* **B409** (1997) 491–498, hep-ph/9704342.

[34] M. A. Braun and G. P. Vacca, "Triple pomeron vertex in the limit N(c) –¿ infinity," *Eur. Phys. J.* **C6** (1999) 147–157, hep-ph/9711486.

[35] L. Lonnblad, "ARIADNE version 4: A Program for simulation of QCD cascades implementing the color dipole model," *Comput. Phys. Commun.* **71** (1992) 15–31.

[36] E. Avsar, G. Gustafson, and L. Lönnblad, "Energy conservation and saturation in small-x evolution," *JHEP* **07** (2005) 062, hep-ph/0503181.

[37] B.-W. Xiao, "On the anomalous dimensions of the multiple pomeron exchanges," *Nucl. Phys.* **A798** (2008) 132–164, arXiv:0710.1922 [hep-ph].

[38] E. Levin and M. Lublinsky, "Balitsky's hierarchy from Mueller's dipole model and more about target correlations," *Phys. Lett.* **B607** (2005) 131–138, hep-ph/0411121.

[39] V. S. Fadin and R. Fiore, "The dipole form of the BFKL kernel in supersymmetric Yang--Mills theories," *Phys. Lett.* **B661** (2008) 139–144, 0712.3901.